Check for updates

International Journal of Climatology

International Journal of Climatology | RMetS

RESEARCH ARTICLE OPEN ACCESS

Assessing Climate Change Impacts on Runoff Variability and Extremes in China Using High-Resolution Simulations

Danyang Gao[1] | Toby Richard Marthews[2] | Guangtao Fu[1] | Li Zhou[3] | Fayyaz Ali Memon[1]

[1]Centre for Water Systems, University of Exeter, Exeter, UK | [2]UK Centre for Ecology & Hydrology (UKCEH), Wallingford, UK | [3]Institute for Disaster Management and Reconstruction, Sichuan University, Chengdu, China

Correspondence: Danyang Gao (dg442@exeter.ac.uk)

Received: 12 May 2025 | **Revised:** 17 November 2025 | **Accepted:** 13 January 2026

Keywords: climate change | CMIP6 | hydrological simulation | land surface model

ABSTRACT

Understanding how climate change influences hydrological variability and extremes is crucial for assessing future hydroclimatic risks and climate adaptation needs. Despite the importance of China as a region highly vulnerable to climate change, few studies have assessed future runoff variability and extremes at a high spatial resolution across the entire country. This study provides a comprehensive analysis of future runoff changes across China at 0.25-degree resolution under medium (SSP245) and high (SSP585) emission scenarios. This analysis uses the Joint UK Land Environment Simulator (JULES), specifically tailored for simulating hydrological processes in China. The model is driven by downscaled and bias-corrected Global Climate Models, using the bias-correction and spatial disaggregation method. Results highlight significant regional disparities in annual runoff, with the Southeast basin experiencing an increase of 41.45 mm/decade under SSP585, compared to a national average increase of 7.30 mm/decade. Seasonal patterns reveal contrasting trends: wetter summers and drier winters are expected in the south, whilst the northwest is expected to experience the opposite pattern. More than 56% of regions, especially in the Pearl River and Southeast basins, are projected to face an increase in extreme high runoff. Extreme low runoff is projected to intensify across over 40% of China, with the central Yangtze River basin being particularly affected. Both extreme high and low runoff are expected to become more severe in the far future, with more severe impacts under SSP585. These findings reveal the spatial differences in runoff changes under climate change, highlighting the varying impacts across different regions and the need for tailored adaptation strategies.

1 | Introduction

Climate change is now having significant impacts on the hydrological cycle in many parts of the world (Yin et al. 2018; Zhang et al. 2018; IPCC 2023). This has resulted in an increase in the likelihood and magnitude of drought and flooding, posing negative impacts on ecology, society and the economy (Schewe et al. 2014; Miller et al. 2021). Therefore, understanding runoff responses to climate change is essential for investigating water security and extreme events. China, one of the most water-stressed nations (Zhai et al. 2022), has a significant mismatch in water resources across regions (Jin et al. 2021). Thus, investigating the climate change impacts on runoff is essential for the sustainable management of water resources in China.

Recent studies have examined runoff responses to climate change across different regions of China using a range of hydrological modelling approaches and climate forcings. Early investigations based on Coupled Model Inter-comparison Project Phase 5 (CMIP5) projections applied models such as VIC-CAS on the Tibetan Plateau to assess changes in runoff components (Zhao et al. 2019), the VIC model for the Upper Yangtze River Basin (Wang et al. 2019), and conceptual hydrological models for 151 catchments across China (Gu et al. 2020). With the

This is an open access article under the terms of the Creative Commons Attribution License, which permits use, distribution and reproduction in any medium, provided the original work is properly cited.

© 2026 The Author(s). *International Journal of Climatology* published by John Wiley & Sons Ltd on behalf of Royal Meteorological Society.

advent of CMIP6 (Eyring et al. 2016), more recent studies have employed both process-based and empirical frameworks to explore runoff changes. These include applications of the Budyko framework to ten major river zones (Guan et al. 2021), the VIC model to eleven major basins (Zhou, Lu, et al. 2023), and various hydrological models applied to individual basins such as the Upper Yellow River Basin (Chen et al. 2023), small basins in the Pearl River Basin (Mo et al. 2023), the Haihe River Basin (Ingabire et al. 2024), and the Liaohe River Basin (Li et al. 2025).

However, the model simulations in these studies were basin-specific and lacked a consistent framework for nationwide hydrological assessment. With 2221 rivers in China having catchment areas exceeding 1000 km^2 (Ministry of Water Resources, P. R. China and National Bureau of Statistics, P. R. China, 2013), achieving comprehensive national coverage is particularly challenging. The difficulty of obtaining hydrologic data in China (Lin et al. 2023), combined with rare observation sites in some regions (e.g., high mountains), makes it extremely difficult to calibrate and validate models for all catchments in China. Moreover, basin-scale studies have reported contrasting results due to differences in model structure, climate forcing, and spatial resolution. Therefore, a substantial gap remains in understanding hydrological changes at a national scale using a unified high-resolution modelling approach.

Some global studies on future runoff under climate change covered China region (Cook et al. 2020; Chai et al. 2021; Wang et al. 2022; Miao et al. 2023). However, their analysis was mainly based on results from CMIP5, CMIP6, Inter-Sectoral Impact Model Inter-Comparison Project (ISMIP2a), and Global Land Data Assimilation System (GLDAS); the resolutions of their runoff projections were coarse ($\geq 0.5°$). Besides, the results were discussed mainly on the continental scale; the specific environmental attributes of China were not particularly addressed. In this study, we will consider the features in the Joint UK Land Environment Simulator (JULES) to simulate hydrological processes with high resolution (0.25°) at the national scale.

The JULES model was developed by the UK Met Office and evolved from the Met Office Surface Exchange Scheme (MOSES, Cox et al. 1999), which was the land surface scheme of the UK Met Office Earth System Model. It is now used as a standalone land surface model to simulate the carbon fluxes (Clark et al. 2011), water, energy, and momentum (Best et al. 2011) between the land surface and the atmosphere. The model has been increasingly used for hydrological assessment (Zulkafli et al. 2013; Le Vine et al. 2016; de la Martínez- Torre et al. 2019; Yang et al. 2019; Chou et al. 2022). However, the application of the JULES model to China needs to be examined, especially for hydrological simulation at high resolutions.

In this study, we apply a high-resolution, nationwide modelling approach to simulate future runoff response to climate change in China. We will answer the following questions: (1) How well can the JULES model simulate hydrological processes in China at 0.25° resolution? (2) What will be the future runoff magnitude, as well as its inter-annual, seasonal variability, and spatial distribution in China? (3) Where and to what extent will China face extreme runoff events under climate change? Addressing these questions will be crucial in enhancing our understanding of hydrological dynamics in China and in formulating effective adaptation and mitigation strategies to reduce the impacts of climate change on water resources management.

2 | Materials and Methods

The overall methodology framework is shown in Figure 1. The framework consists of three main components: driving data

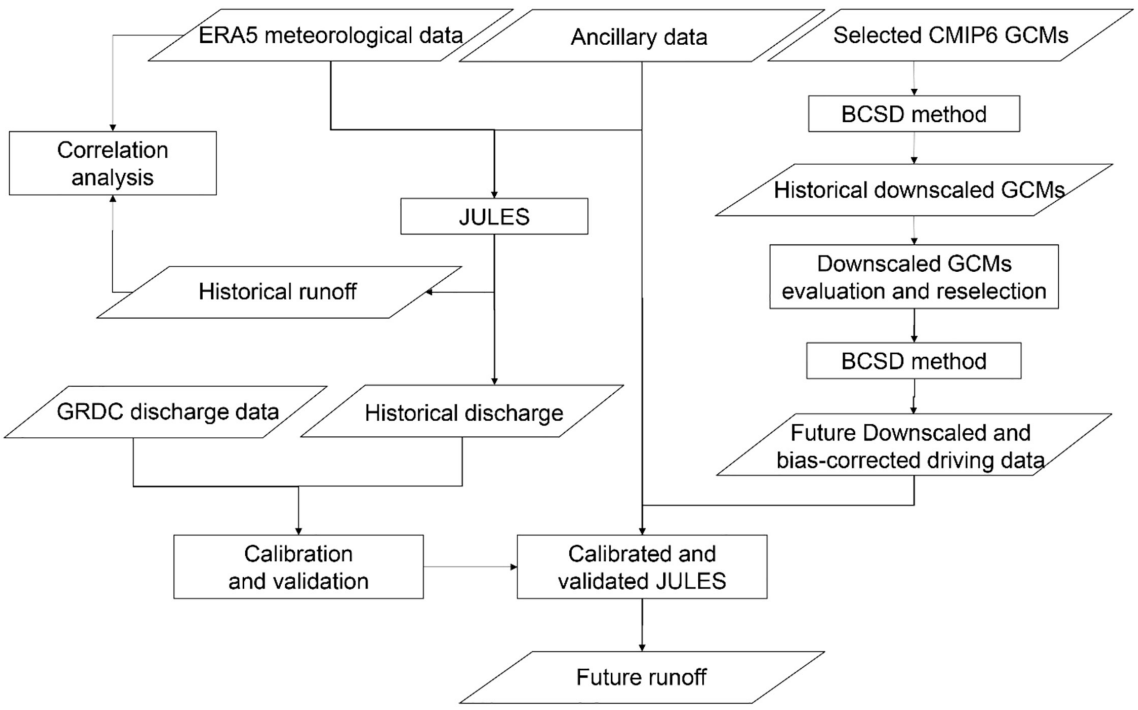

FIGURE 1 | Flowchart of the methodological framework.

10970088, 0, Downloaded from https://rmets.onlinelibrary.wiley.com/doi/10.1002/joc.70270 by UK Centre For Ecology & Hydrology, Wiley Online Library on [30/01/2026]. See the Terms and Conditions (https://onlinelibrary.wiley.com/terms-and-conditions) on Wiley Online Library for rules of use; OA articles are governed by the applicable Creative Commons License

preparation, model calibration and validation, and future runoff projection. ERA5 meteorological data were first used to drive the JULES model for historical simulations, supported by ancillary datasets. The simulated historical discharge was evaluated against observed discharge data from the Global Runoff Data Centre (GRDC) for model calibration and validation. Meanwhile, a set of CMIP6 global climate models (GCMs) was selected and bias-corrected using the Bias Correction and Spatial Disaggregation (BCSD) method to produce downscaled meteorological inputs. The downscaled GCMs were evaluated, and the best-performing models were reselected to generate the final bias-corrected driving data for future simulations. The calibrated and validated JULES model was then forced with these downscaled future climate data to produce high-resolution projections of future runoff across China.

2.1 | The JULES Model

To accurately simulate hydrological processes, we employed the JULES model, which requires both meteorological forcing data and ancillary data. The following describes the configuration and process for historical simulation, including the calibration and validation of the model using observed discharge data.

Input for the JULES model includes meteorological forcing data and ancillary data. In its standard configuration, JULES recognises nine land cover types: broadleaf trees, needleleaf trees, C_3 (temperate) grass, C_4 (tropical) grass, shrubs, urban, inland water, bare soil and ice (Best et al. 2011). In this study, historical meteorological forcing data include near surface temperature, precipitation, downward shortwave and longwave radiation, wind speed, specific humidity and surface pressure from the European Centre for Medium-Range Weather Forecasts Reanalysis 5 (ERA5, Hersbach et al. 2020). The ancillary data are from Marthews et al. (2022), considering nine land cover and seven soil layers.

To generate a reasonable initial condition, the JULES model was spun up in December of 1959 with 200 spin up cycles. The main run was during 1960 to 2014 covering all of China, using 0.25° resolution and a daily timestep. Observed discharge from the Global Runoff Data Centre (GRDC) was used to do monthly calibration and validation (Figure 2). The model calibration was from 1962 to 1977; 1978 to 1986 were used for validation. The Pearson correlation coefficient (r), Nash-Sutcliffe efficiency coefficient (NSE, Nash and Sutcliffe 1970), Kling-Gupta efficiency (KGE, Gupta et al. 1999), ratio of the root mean square error to the standard deviation of the measured data (RSR, Murphy et al. 2004), and the percent bias (PBIAS, Gupta et al. 1999) were used to evaluate the model performance. The corresponding equations are shown in Equations (1–5). The values of r, NSE, and KGE should all be 1 in an ideal model, whereas RSR and PBIAS should be 0. Generally, an NSE greater than 0.5 indicates good alignment (Decharme et al. 2012). More detailed standard thresholds for NSE are provided in Marthews et al. (2022) and descriptions of these performance metrics are provided in Singh et al. (2023).

FIGURE 2 | Location of GRDC stations for calibration and validation. [Colour figure can be viewed at wileyonlinelibrary.com]

10970088, 0, Downloaded from https://rmets.onlinelibrary.wiley.com/doi/10.1002/joc.70270 by UK Centre For Ecology & Hydrology, Wiley Online Library on [30/01/2026]. See the Terms and Conditions (https://onlinelibrary.wiley.com/terms-and-conditions) on Wiley Online Library for rules of use; OA articles are governed by the applicable Creative Commons License

$$r = \frac{n \sum Q_o Q_m - \left(\sum Q_o\right)\left(\sum Q_m\right)}{\sqrt{\left[n \sum \left(Q_O\right)^2 - \left(\sum Q_O\right)^2\right]\left[n \sum \left(Q_m\right)^2 - \left(\sum Q_m\right)^2\right]}} \quad (1)$$

$$\mathrm{NSE} = 1 - \frac{\sum_{t=1}^{T}\left(Q_o^t - Q_m^t\right)^2}{\sum_{t=1}^{T}\left(Q_o^t - \overline{Q}_o\right)^2} \quad (2)$$

$$\mathrm{KGE} = 1 - \sqrt{(r-1)^2 + \left(\frac{\sigma_p}{\sigma_{ob}} - 1\right)^2 + \left(\frac{Q_m}{Q_o} - 1\right)^2} \quad (3)$$

$$\mathrm{RSR} = \frac{\sqrt{\sum_{t=1}^{T}\left(Q_o - Q_m\right)^2}}{\sigma_{ob}} \quad (4)$$

$$\mathrm{PBIAS} = \left[\frac{\sum_{t=1}^{T}\left(Q_o - Q_m\right)}{\sum_{t=1}^{T}\left(Q_o\right)}\right] \times 100 \quad (5)$$

where Q_m is modelled discharge, Q_o is observed discharge, $\overline{Q}_o$ is the mean of observed discharges, σ_{ob} and σ_p refer to the standard deviation of the observed and modelled discharge, respectively. t is time, and n is the number of observations available for analysis.

2.2 | Bias-Correction Spatial Disaggregation (BCSD) Method

To drive the JULES model for future runoff simulations, it is necessary to prepare future climate data at 0.25° resolution. To achieve this, we used the bias-correction and spatial disaggregation (BCSD) method (Wood et al. 2004; Thrasher et al. 2022) for downscaling data from CMIP6 GCMs, as detailed below.

The BCSD method compares the original GCMs output with climate observations during a common historical reference period and uses the information obtained from the comparison to adjust future projections of GCMs, aiming to align the GCMs more closely with historical observation data and enhance their realism within the specific spatial area (Thrasher et al. 2022).

The BCSD method consists of three steps: preprocessing, bias correction, and spatial disaggregation. Preprocessing is only for the temperature variable; the main purpose is to detrend temperature so that their climate trends would not be affected by the bias correction. The 9-year moving average is calculated in each month individually. These trends are preserved and then reincorporated into the adjusted data following the bias correction process. The bias correction process corrects the bias in GCMs output by observations; firstly, ERA5 datasets were interpolated to match the resolution of the selected GCMs. The data within ±15-day window from GCMs and ERA5 in a reference period from 1959 to 2014 were chosen to generate two cumulative distribution functions (CDFs). The quantile corresponding to each original GCM value was derived from the GCM-based CDF distribution for that particular day. Subsequently, this quantile was used to calculate the corresponding value from the ERA5-based CDF distribution. The final value is the bias-corrected GCMs data. Spatial disaggregation process interpolates the bias-corrected GCMs data to the observational resolution (0.25°). A smoothed daily climatology was generated over the reference period based on ERA5 by a Fast Fourier Transform retaining three harmonics. This climatology was then interpolated to the original grid of the GCMs and factored out of the bias-corrected GCMs either by subtracting from the temperature variables or by dividing from the other variables. The residual fields were bilinearly interpolated to the original 0.25° grid of the ERA5. Subsequently, the 0.25° climatology was factored back in either through addition to the temperature variables or multiplication by the other variables, yielding the final downscaled GCMs data.

We selected six GCMs from CMIP6 (EC-Earth3, INM-CM5-0, MIROC6, MPI-ESM1-2-HR, MRI-ESM2-0 and NorESM2-LM, shown in Table S1) based on their documented performance and frequent use in studies over China. Previous evaluations show that EC-Earth3 and MPI-ESM1-2-HR rank highly for both temperature and precipitation across seasons, whilst MRI-ESM2-0 and NorESM2-LM perform well at an annual scale (Yang et al. 2021). Basin-scale assessments further indicate that all six models simulate temperature reliably, and EC-Earth3, MPI-ESM1-2-HR, MRI-ESM2-0 and NorESM2-LM capture realistic precipitation variability in most regions. MIROC6 performs well in the Yellow River and Southwest regions, and INM-CM5-0 shows comparatively good precipitation performance in the Northeast (Lu et al. 2022). Uncertainty decomposition also demonstrates that these models contribute meaningfully to the structural spread of CMIP6 projections, with EC-Earth3 and MPI-ESM1-2-HR dominant across all regions, and the others adding regional structural diversity (Jia et al. 2023). Moreover, these six models are widely used in runoff projection studies over China (e.g., Bian et al. 2021; Wang et al. 2022; Zhou, Lu, et al. 2023; Ingabire et al. 2024; Song et al. 2024; Xue et al. 2024).

First, we downscaled the precipitation of these six GCMs. By comparing the temporal root-mean-square error (RMSE) of annual precipitation in the reference period over China, spatial Pearson correlation coefficient (r), and RMSE for multi-year average (1959–2014) daily precipitation, the three best performing GCMs were selected. To ensure the selected GCMs represent the performance of most GCMs, daily average precipitation and temperature from 1959 to 2014 for the selected GCM ensemble means were compared with the ensemble means of 19 GCMs. These GCMs include ACCESS-CM2, ACCESS-ESM1-5, CanESM5, CMCC-ESM2, CNRM-ESM2-1, EC-Earth3, EC-Earth3-Veg, FGOALS-g3, GFDL-ESM4, INM-CM4-8, INM-CM5-0, MIROC-ES2L, MPI-ESM1-2-HR, MPI-ESM1-2-LR, MRI-ESM2-0, NorESM2-LM, NorESM2-MM, TaiESM1, and UKESM1-0-LL.

Then we downscaled the near surface temperature, precipitation, downward shortwave and longwave radiation, wind speed,

10970088, 0, Downloaded from https://rmets.onlinelibrary.wiley.com/doi/10.1002/joc.70270 by UK Centre For Ecology & Hydrology, Wiley Online Library on [30/01/2026]. See the Terms and Conditions (https://onlinelibrary.wiley.com/terms-and-conditions) on Wiley Online Library for rules of use; OA articles are governed by the applicable Creative Commons License

specific humidity, and surface pressure of these three GCMs in middle and high emission scenarios (SSP245 and SSP585) as future input forcing data for the JULES model.

2.3 | Future Projection Under Climate Change

With the validated JULES model and downscaled future climate data established, the next phase involved projecting future hydrological processes under a range of climate change scenarios. This section details how these projections were made using the JULES model and the evaluation of future runoff dynamics and variability.

The downscaled GCMs for both the historical and future periods under the two scenarios were input into the calibrated and validated JULES model to simulate the hydrological processes. The runoff rate output by JULES is in units of $kg{\cdot}m^{-2}{\cdot}s^{-1}$. We estimated the runoff at different time steps, measured in mm of depth. The annual and seasonal variations in runoff over China and its basins were analysed using the Mann-Kendall test (Mann 1945; Kendall 1975) to assess changing trends. Runoff variability was evaluated by calculating the Detrended Standard Deviation (DSD). This involved first detrending the time series data to remove long-term trends, followed by computing the standard deviation of the residuals to quantify the magnitude of inter-annual fluctuations.

To assess changes in extreme runoff under climate change, the future period was divided into the near future (2021–2060) and the far future (2061–2100). The 90th and 10th percentile runoff values were calculated for each grid in China during the historical period (1975–2014), as well as for the near and far future under SSP245 and SSP585 scenarios.

3 | Results

3.1 | JULES Model and Downscaled GCMs Evaluation

The JULES model was calibrated and validated against observed discharge from GRDC stations across China. The results show that the model reproduces historical hydrological processes well, with satisfactory performance across multiple evaluation metrics (Figures S1 and S2, Table S2). Higher skill is found in humid regions of southern China, reflecting the model's ability to capture regional hydrological variability. Additional correlation analyses between simulated runoff and observed climate variables (Figure S3) further confirm the physical consistency of the modelled runoff responses to temperature and precipitation. Detailed analyses are provided in the Supporting Information.

The bias-corrected and downscaled GCMs produced using the BCSD method also show markedly improved consistency with ERA5 reanalysis data, confirming the reliability of the driving climate inputs. The Taylor diagram (Figure 3) illustrates the overall agreement of bias-corrected precipitation from the six selected GCMs with ERA5 in terms of correlation, standard deviation, and centred RMSE. All models show high correlations ($r > 0.9$) and standard deviations close to 1, indicating that the

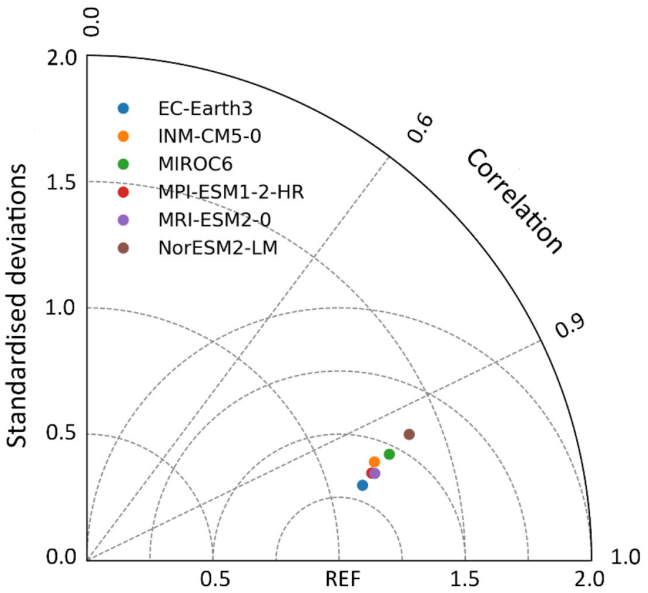

FIGURE 3 | Taylor diagram showing the performance of bias-corrected precipitation from the six selected CMIP6 GCMs compared with ERA5. [Colour figure can be viewed at wileyonlinelibrary.com]

BCSD method effectively reduces systematic biases and enhances the consistency amongst models. The close clustering of all GCMs around the reference point also suggests that inter-model differences are minimal after bias correction, implying that subsequent hydrological projections are less sensitive to the choice of individual GCMs. Detailed evaluation metrics and bias comparison analyses for each GCM and meteorological variable are provided in Table S3 and Figures S4–S8.

3.2 | Future Runoff Simulation

3.2.1 | Inter-Annual Changes and Variability

The calibrated and validated JULES model is used to project runoff changes in China under SSP245 and SSP585. The Mann-Kendall test reveals a significant upward trend expected in runoff under the high-emission scenario (SSP585), with an increase of 7.30 mm per decade from 2015 to 2100. In contrast, no clear trend is expected under SSP245 (Figure 4a). This projected runoff increase under SSP585 aligns with a significant rise in precipitation (+21.44 mm per decade, Figure 4b), although the growth in runoff is moderated by a concurrent rise in evapotranspiration (+13.19 mm per decade, Figure 4c).

From the perspective of variability, The Detrended Standard Deviation (DSD) reveals that both precipitation and runoff variability are projected to increase significantly under SSP585, with increases of 37% and 35% respectively, compared to the historical period (1962–2014). In contrast, under SSP245, the increases are more moderate, at 29% and 26% respectively, compared to the historical baseline. This highlights a greater likelihood of hydrological extremes under SSP585. Conversely, the variability in evapotranspiration remains relatively stable, showing a slight decrease of 6% in SSP scenarios compared to the historical period. Overall, whilst evapotranspiration rates

10970088, 0, Downloaded from https://rmets.onlinelibrary.wiley.com/doi/10.1002/joc.70270 by UK Centre For Ecology & Hydrology, Wiley Online Library on [30/01/2026]. See the Terms and Conditions (https://onlinelibrary.wiley.com/terms-and-conditions) on Wiley Online Library for rules of use; OA articles are governed by the applicable Creative Commons License

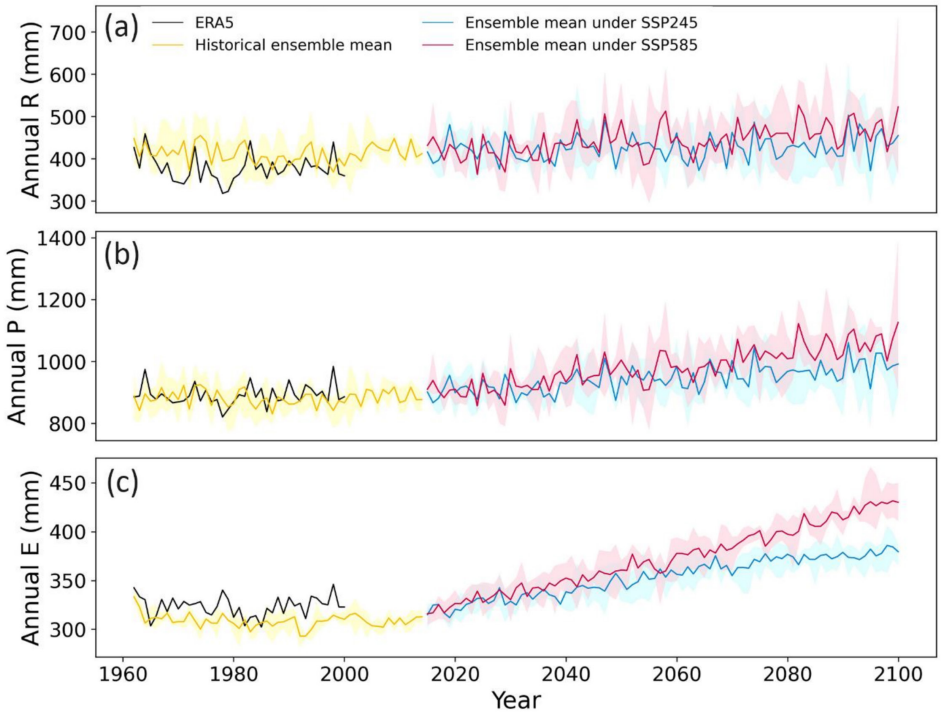

FIGURE 4 | Projected annual hydrological changes across China in the historical period and under SSP245 and SSP585 scenarios. (a) Runoff depth, (b) Precipitation, and (c) Evapotranspiration. The black line represents the precipitation from ERA5, the simulated runoff and evapotranspiration based on ERA5. The yellow, blue and red lines are the ensemble mean precipitation from the three GCMs, simulated runoff and evapotranspiration driving by the three GCMs in historical, under SSP245 and SSP585, respectively. The shaded areas indicate the range between the maximum and minimum values of precipitation, simulated runoff depth and evapotranspiration based on the three GCMs. [Colour figure can be viewed at wileyonlinelibrary.com]

are expected to rise (Figure 4c), their fluctuations will remain consistent, contributing less uncertainty compared to precipitation and runoff.

In summary, under SSP585, a combination of increased precipitation and runoff variability points to heightened hydrological risks, whereas a more stable hydrological response is expected under SSP245, though with variability greater than in the historical period.

From a regional perspective, the projected annual runoff changes show significant spatial differences across basins (Figure 5a). Under SSP585, annual runoff is expected to increase notably in eastern and southern basins, including the Haihe River, Huaihe River, Pearl River, Songhua River, Southeast, and Southwest basins. Amongst these, the Southeast basin is expected to exhibit the most dramatic increase, with a trend rate of 41.45 mm per decade, driven by a substantial precipitation increase of 59.38 mm per decade. Under SSP245, the trends in most basins are expected to be less dramatic compared to SSP585, but the direction of change is expected to be the same as under SSP585.

The DSD of annual runoff across basins in China highlights increasing variability under future climate scenarios (Figure 5b). Notably, the Pearl River basin is expected to show a significant increase in DSD, rising by 35% under SSP245 and 59% under SSP585 compared to historical (1962–2014) levels, reflecting its susceptibility to substantial fluctuations and indicating a growing risk of extreme runoff events in this region. In contrast, the Continental and Southwest basin shows decreasing trends in DSD, with reductions of 13% under SSP245 and 14% under SSP585, reflecting their relative stability.

3.2.2 | Seasonal Changes and Variability

From the perspective of seasonal runoff, spring and summer runoff is projected to increase under both scenarios (Figure 6b,c). Notably, the summer runoff under SSP585 is expected to rise at a significantly higher rate (4.60 mm/decade) compared to SSP245 (0.82 mm/decade), indicating a significant humidification trend. In contrast, winter runoff is projected to show a decreasing trend, suggesting the potential for drier conditions (Figure 6a). This decrease is expected to be more significant under SSP585, highlighting the potential risk of reduced water resources during winter.

Runoff is projected to increase in summer across eight basins, with the highest increases expected in the Southeast basin, at 34.27 mm per decade (Figure 7a). However, in the Continental basin, summer runoff is expected to decrease by 0.90 mm and 1.34 mm per decade under SSP245 and SSP585, respectively, whilst winter runoff is expected to increase by 0.11 and 0.13 mm per decade under the same scenarios. In contrast, southern basins, including the Pearl River, Southeast, and Yangtze River basins, are projected to experience decreasing winter runoff, with higher rates of 1.95, 2.32, and 1.22 mm per decade under SSP585, respectively.

10970088, 0, Downloaded from https://rmets.onlinelibrary.wiley.com/doi/10.1002/joc.70270 by UK Centre For Ecology & Hydrology, Wiley Online Library on [30/01/2026]. See the Terms and Conditions (https://onlinelibrary.wiley.com/terms-and-conditions) on Wiley Online Library for rules of use; OA articles are governed by the applicable Creative Commons License

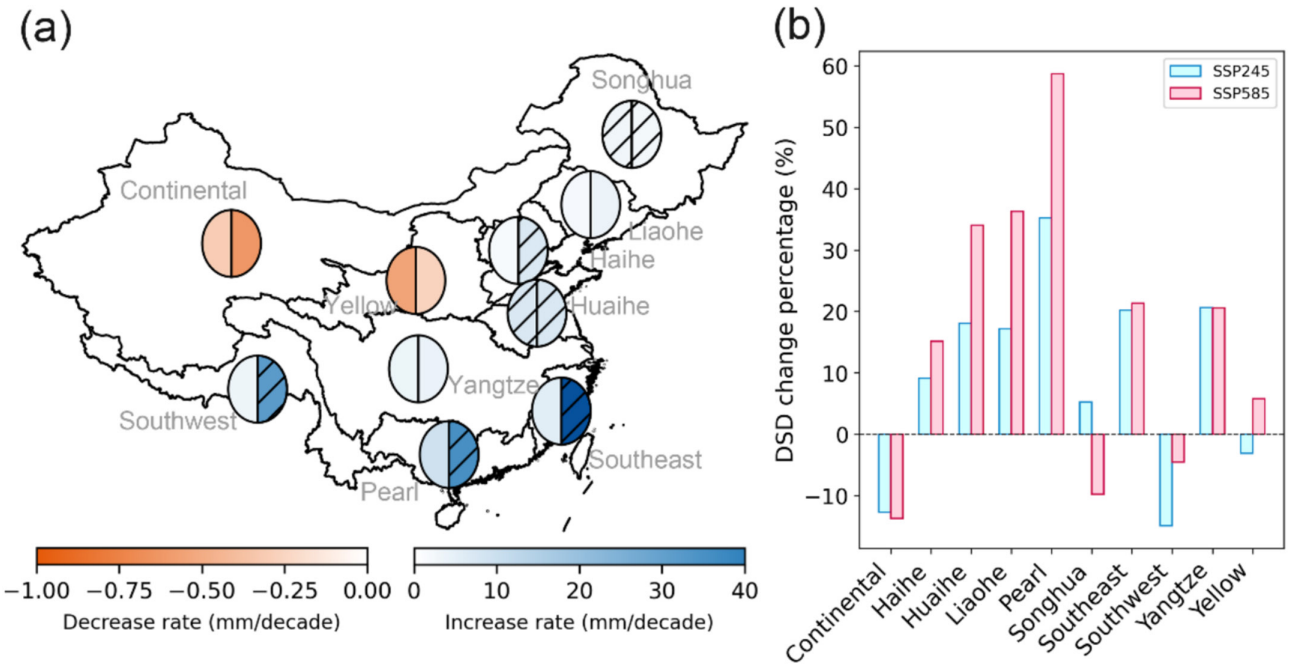

FIGURE 5 | Rate of annual runoff depth change during 2015 to 2100 under SSP245 and SSP585. (a) and percentage change in Detrended Standard Deviation under SSP245 and SSP585 compared to historical levels (b) in each basin. In (a), the left semicircle represents SSP245, the right semicircle represents SSP585. Slashed lines indicate trends that have passed the Mann-Kendall test. Detailed numerical values are listed in Table S4. [Colour figure can be viewed at wileyonlinelibrary.com]

Seasonal variability in these basins is expected to follow a similar pattern (Figure 7b). In the Continental basin, winter runoff is projected to show an increase in DSD by 33% and 52% under SSP245 and SSP585, respectively, compared to historical levels, whilst the variability of summer runoff is projected to decrease. Conversely, in the Pearl River, Southeast, and Yangtze River basins, summer runoff is expected to exhibit greater variability compared to winter runoff, with the highest increase of 70% projected for the Pearl River basin under SSP585.

These trends suggest a stark contrast in the seasonal runoff patterns between northwestern and southern China. Southern China is expected to experience wetter summers and drier winters, with the increase in winter runoff variability further emphasising the potential for more unpredictable water availability during this season. In contrast, the opposite trend—wetter winters and drier summers—is expected in northwestern China, with increased summer runoff variability indicating a higher likelihood of frequent or severe fluctuations. These changes could exacerbate flooding risks and pose significant challenges for water management strategies in the region.

3.3 | Projected Changes in Extreme Runoff

Extreme high and low runoff events play a critical role in assessing future flood and drought risks. To capture these changes, we analysed the 90th percentile (high flow) and 10th percentile (low flow) runoff as indicators of flood and drought conditions, respectively. These metrics provide an effective proxy for understanding how the frequency and intensity of hydrological extremes may evolve under different climate scenarios.

3.3.1 | Changes in Extreme High Runoff

Extreme runoff changes reveal distinct patterns across basins and future scenarios. Spatial changes in 90th percentile runoff are shown in Figure 8, highlighting regions with heightened extreme high runoff, which may indicate an increased flood risk. The basin mean values, percentage changes and the proportion of area with positive changes in each basin are presented in Tables S6–S8. Compared to the historical period, more than 56% of area in China, particularly those in southern China, are projected to experience increased extreme high runoff in the future. The high flow is projected to increase most prominently in southern basins under SSP585, particularly in the Pearl River (by +0.37 mm/day in NF and +1.03 mm/day in FF relative to the historical period; equivalent to increases of 5.92% and 16.33%, respectively) and Southeast Basin (by +0.42 mm/day in NF and +1.03 mm/day in FF; 5.89% and 14.23%), indicating a higher potential for extreme flooding events over time. In contrast, the Continental Basin and Songhua River Basin show comparatively minor changes in high flows, suggesting a relatively stable flood risk in these regions.

Under SSP245 (Figure 8a,d), notable increases are projected in the western Pearl River basin, the Southwest basin, and the middle Yangtze River basin. In these regions, more than 61% of area is projected to experience an increase in 90th percentile runoff. These increases are expected to become more pronounced in the far future compared to the near future, particularly in the Southwest and Yangtze River basins, where the increases in maximum 90th percentile runoff are projected to reach 65% and 56%, respectively.

Under SSP585 (Figure 8b,e), the extent and intensity of increased 90th percentile runoff are more significant in the

10970088, 0, Downloaded from https://rmets.onlinelibrary.wiley.com/doi/10.1002/joc.70270 by UK Centre For Ecology & Hydrology, Wiley Online Library on [30/01/2026]. See the Terms and Conditions (https://onlinelibrary.wiley.com/terms-and-conditions) on Wiley Online Library for rules of use; OA articles are governed by the applicable Creative Commons License

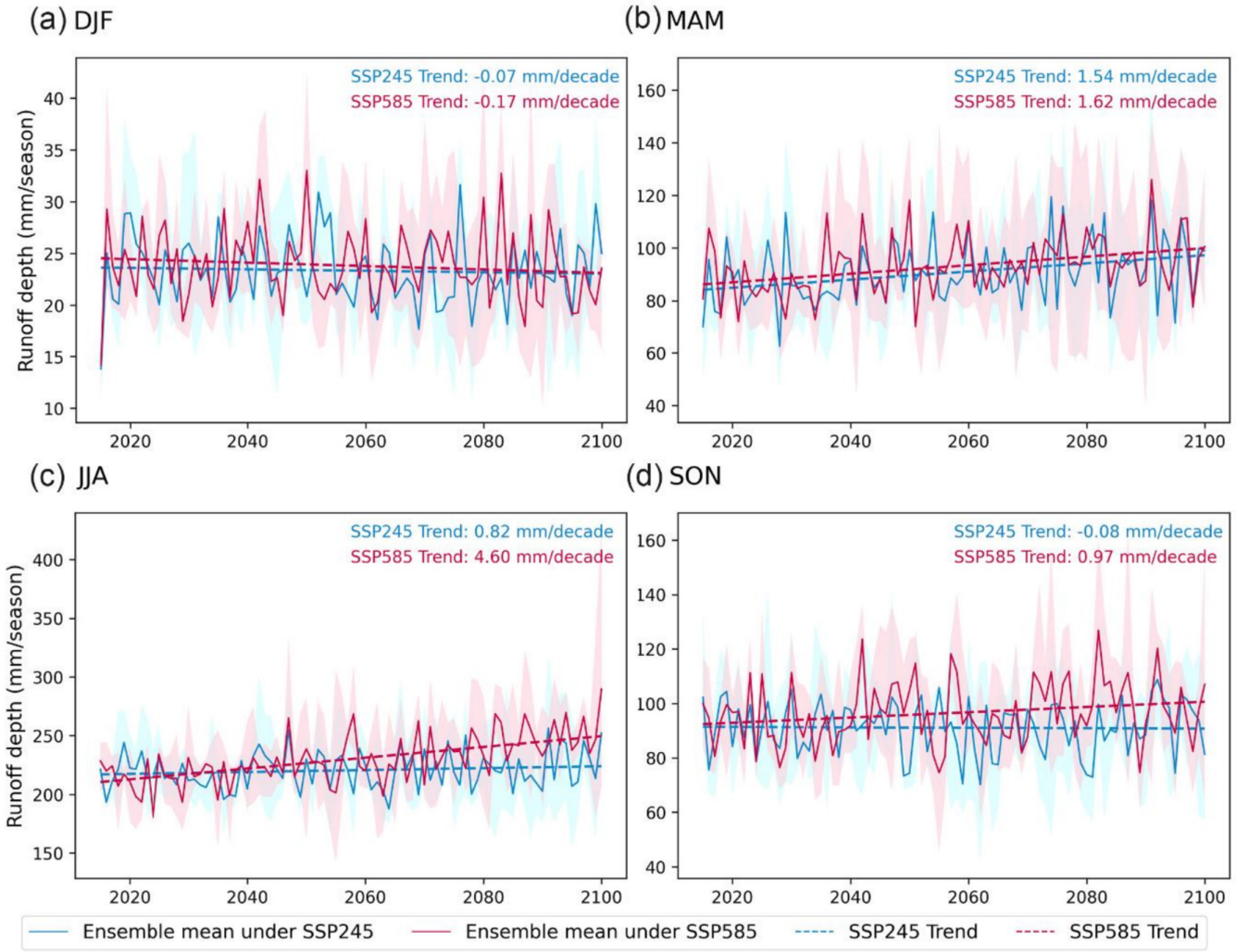

FIGURE 6 | Seasonal runoff depth over China. The blue and red lines represent the ensemble mean of simulated runoff driven by three GCMs under SSP245 and SSP585, respectively. The shaded areas indicate the range between the maximum and minimum simulated runoff depths across the three GCMs. The blue and red dashed lines represent the runoff trends under SSP245 and SSP585, respectively, with the rates of change indicated in the top right corner. [Colour figure can be viewed at wileyonlinelibrary.com]

southern basins (Southeast, Pearl River, and Yangtze River basins) in the far future, with the basin mean increase surpassing 141% compared to the near future. Additionally, the maximum 90th percentile runoff in these basins is projected to increase by more than 86%, signalling a significantly heightened extreme high runoff.

Compared to SSP245, southern regions (Pearl River, Southeast, and Southwest basins) are projected to experience a lower risk of extreme high runoff in the near future under SSP585 but a significantly higher risk in the far future. In the near future, the basin mean 90th percentile runoff under SSP585 is expected to be lower than SSP245 by less than 0.06 mm/day in the Southeast and Southwest basins, whilst in the Pearl River basin, it is expected to be slightly higher by more than 0.06 mm/day (Figure 8c). However, in the far future, the basin mean 90th percentile runoff under SSP585 is projected to increase substantially in all three basins, with the runoff expected to exceed SSP245 by more than 0.50 mm/day (Figure 8f). In the near future, less than 59% of area in these basins is expected to experience an increase in 90th percentile runoff under SSP585 compared to SSP245. In contrast, in the far future, more than 90% of area is projected to experience an increase in 90th percentile runoff, signalling a sharp rise in the risk of extreme high runoff under SSP585.

3.3.2 | Changes in Extreme Low Runoff

Figure 9 illustrates the spatial patterns of 10th percentile runoff, providing insights into extreme low runoff, which may indicate an increased drought risk under SSP245 and SSP585. The basin mean values, percentage changes and the proportion of area with negative changes in each basin are presented in Tables S9–S11. In both scenarios, for both the near and the far future, a decrease in the 10th percentile runoff is expected across more than 40% of grid cells in China, primarily concentrated in central and southern China. Substantial declines are projected in southern basins, particularly in the Pearl River (by −0.02 mm/day in NF and −0.05 mm/day in FF relative to the historical period; −22% and −50%, respectively) and Southeast Basin (by −0.03 mm/day in NF and −0.07 mm/day in FF; −16% and −34%), indicating heightened drought vulnerability. In

10970088, 0, Downloaded from https://rmets.onlinelibrary.wiley.com/doi/10.1002/joc.70270 by UK Centre For Ecology & Hydrology, Wiley Online Library on [30/01/2026]. See the Terms and Conditions (https://onlinelibrary.wiley.com/terms-and-conditions) on Wiley Online Library for rules of use; OA articles are governed by the applicable Creative Commons License

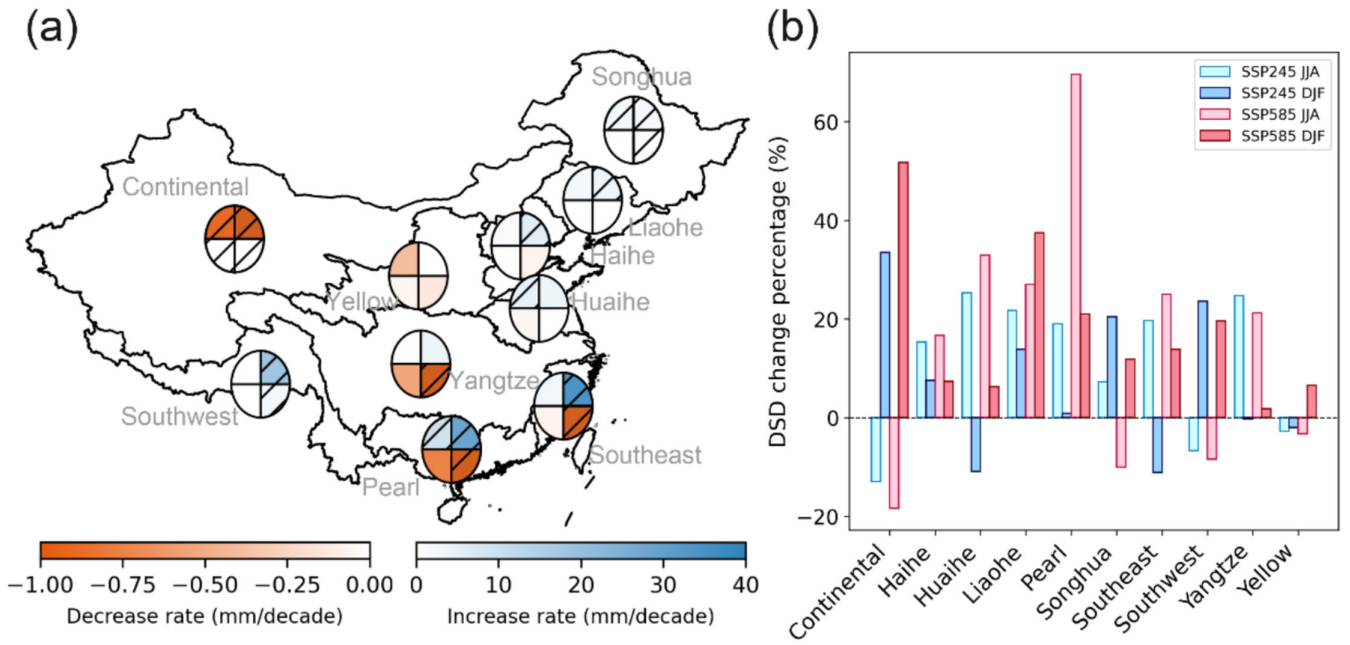

FIGURE 7 | Rate of JJA and DJF runoff depth change from 2015 to 2100 under SSP245 and SSP585 (a) and the percentage change in Detrended Standard Deviation under SSP245 and SSP585 compared to historical levels (b) in each basin. In (a), the left semicircle represents SSP245, the right semicircle represents SSP585, the top semicircle represents JJA, and the bottom semicircle represents DJF. Slashed lines indicate trends that have passed the Mann-Kendall test. Detailed numerical values are listed in Table S5. [Colour figure can be viewed at wileyonlinelibrary.com]

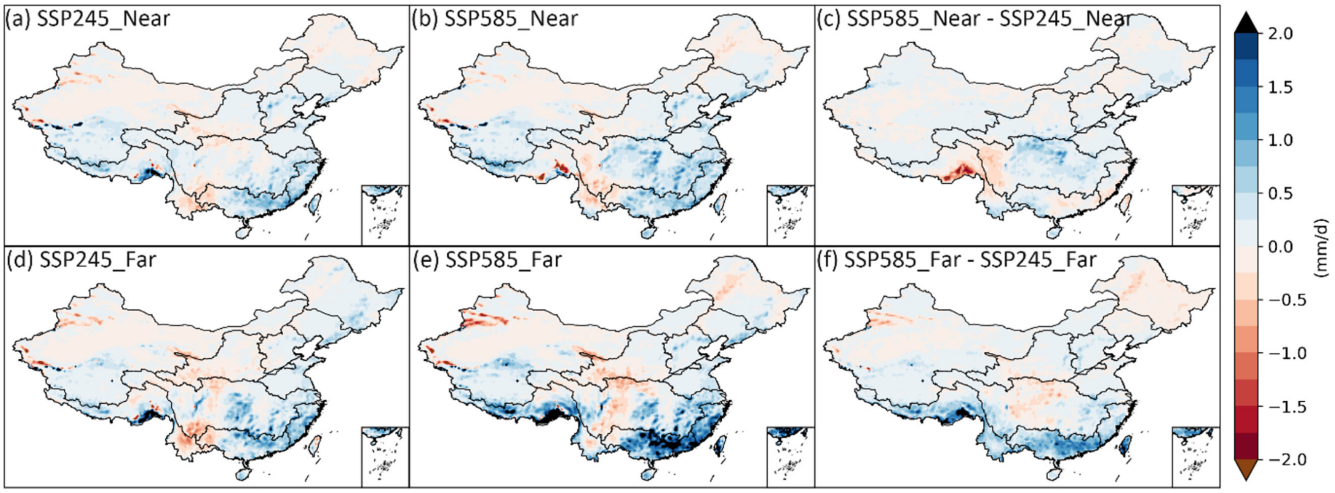

FIGURE 8 | Multi-year ensemble mean 90th percentile runoff changes in (a) 2021–2060 and (d) 2061–2100 under the SSP245, as well as (b) 2021–2060 and (e) 2061–2100 under the SSP585, relative to the historical period (1975–2014). (c) and (f) are the differences in multi-year ensemble mean 90th percentile runoff depth between SSP245 and SSP585 in 2021–2060 and 2061–2100, respectively. [Colour figure can be viewed at wileyonlinelibrary.com]

contrast, northwestern basins, especially the Continental Basin, are projected to experience modest increases (by +0.0034 mm/day in NF and +0.0059 mm/day in FF; 31% and 53%), suggesting improved baseflow conditions.

Under SSP245 (Figure 9a,d), the most significant reductions in low flows are expected in the southern Yangtze and northern Pearl River basins. The minimum 10th percentile runoff is projected to decrease by more than 0.20 mm/day in the near future and by over 0.28 mm/day in the far future, compared to the historical period, indicating a more significant reduction in the far future.

Similarly, under SSP585 (Figure 9b,e), a similar drying pattern is expected, with the trend projected to intensify further in southern China. In the far future, over 82% of area in the Southeast, Yangtze, and Pearl River basins are projected to face decreased low flows. Notably, a more significant decline is expected in the central Yangtze River basin, with the minimum 10th percentile runoff decreasing by 0.32 mm/day compared to the near future.

In the near future (Figure 9c), only 33% of grid cells in China are projected to experience a reduction in the 10th percentile runoff under SSP585 compared to SSP245, whilst in the far future, the percentage is expected to increase to 44%. This

10970088, 0, Downloaded from https://rmets.onlinelibrary.wiley.com/doi/10.1002/joc.70270 by UK Centre For Ecology & Hydrology, Wiley Online Library on [30/01/2026]. See the Terms and Conditions (https://onlinelibrary.wiley.com/terms-and-conditions) on Wiley Online Library for rules of use; OA articles are governed by the applicable Creative Commons License

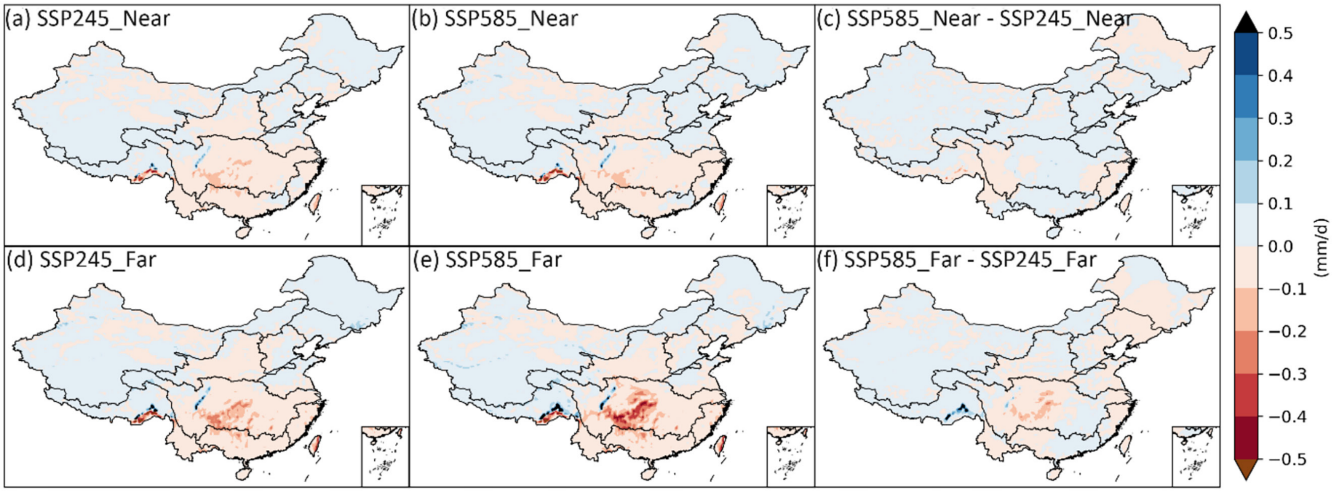

FIGURE 9 | Multi-year ensemble mean 10th percentile runoff changes in (a) 2021–2060 and (d) 2061–2100 under the SSP245, as well as (b) 2021–2060 and (e) 2061–2100 under the SSP585, relative to the historical period (1975–2014). (c) and (f) are the differences in multi-year ensemble mean 10th percentile runoff depth between SSP245 and SSP585 in 2021–2060 and 2061–2100, respectively. [Colour figure can be viewed at wileyonlinelibrary.com]

indicates that the area facing extreme low runoff is expected to be wider under SSP245 in the near future, but under SSP585, the drying trend is expected to intensify over time. Notably, in the far future (Figure 9f), the minimum 10th percentile runoff in the Yangtze River is expected to decrease by 0.28 mm/day under SSP585 compared to SSP245. This suggests that under high emission scenarios, specific regions, such as the central Yangtze River basin, are expected to face more severe extreme low runoff.

Overall, these findings indicate that focusing solely on mean annual runoff may obscure critical changes in extreme flows. Highlighting both low and high flow changes, as well as their evolution from the near future to the far future, is therefore essential for understanding hydrological risks and planning water resources management under future climate scenarios.

4 | Discussion

4.1 | Comparisons of Runoff Estimates in Different Studies

The change trends in annual runoff depth over China are similar to the results in Zhou, Lu, et al. (2023), indicating an overall wavelike rise, with the upward trend under SSP585 expected to be more severe than that under SSP245. However, the rise in runoff depth under SSP245 in this study does not pass the significance test in the Mann-Kendall trend test. In Guan et al. (2021), the increase in runoff in 10 typical basins in China under SSP585 is not consistently greater than that under SSP245. This is attributed to Guan et al. (2021) using the climate elasticity method to project future runoff, which ignores complex hydrological and ecological processes.

The magnitude of simulated runoff depth in this study is larger than that in Zhou, Lu, et al. (2023). On one hand, the difference of simulated runoff depth may be caused by using different models and parameterisation schemes. On the other hand, it is mainly because the GCMs downscaled and historical hydrological modelling in this study are based on ERA5. ERA5 generally overestimates precipitation in the northern and western regions of China, but it can capture seasonal variations and the broad spatial distributions in both magnitudes and trends (Sun et al. 2021; Zhou, Chen, et al. 2023). We used three meteorological datasets to drive the model, including ERA5. Our evaluation showed that ERA5 performed the best compared to the other datasets. We agree with other scholars that, despite its biases, ERA5 remains one of the best reanalysis datasets available, providing a comprehensive set of variables (Cucchi et al. 2020; Xu et al. 2021).

The spatial variations of projected runoff in this study are similar to those in other studies (Cook et al. 2020; Wang et al. 2022; Zhou, Lu, et al. 2023). However, Cook et al. (2020) and Wang et al. (2022) analysed runoff change by percentage change, which cannot visually convert the actual changes in runoff volume. The percentage change in runoff is expected to be the largest in northern China, which could mislead readers into thinking that northern China is projected to face the most dramatic change in absolute runoff volume. However, the combined volume of runoff from six northern river basins, covering a total catchment area of 2.27 million km^2, contributes to less than 20% of the national total runoff. In contrast, four southern river basins, spanning a total catchment area of 2.86 million km^2, contribute to over 80% of the national total runoff (Zhang et al. 2011; Yang et al. 2022). Additionally, the runoff analysis in Cook et al. (2020) and Wang et al. (2022) was based on global coarse resolution and did not focus on the changes within China. Seasonal changes and changes in extreme runoff were not included in these studies (Cook et al. 2020; Wang et al. 2022; Zhou, Lu, et al. 2023).

Beyond the annual changes, our results highlight that seasonal shifts in runoff need to be interpreted in the context of annual trends. Under SSP585, the projected overall increase in annual

10970088, 0, Downloaded from https://rmets.onlinelibrary.wiley.com/doi/10.1002/joc.70270 by UK Centre For Ecology & Hydrology, Wiley Online Library on [30/01/2026]. See the Terms and Conditions (https://onlinelibrary.wiley.com/terms-and-conditions) on Wiley Online Library for rules of use; OA articles are governed by the applicable Creative Commons License

runoff is primarily driven by the significant summer increase, whilst the simultaneous decline in winter runoff is expected to partly offset this rise. This indicates that the annual upward trend is unlikely to translate into uniformly improved water availability but will instead intensify the seasonal contrast between wet and dry periods in southern China. In contrast, in northwestern China, the relatively small annual changes are projected to mask a redistribution within the year, with wetter winters but drier summers. These findings suggest that focusing only on annual projections may obscure critical seasonal dynamics, underscoring the importance of jointly considering both annual and seasonal scales when assessing future hydrological risks and water security.

4.2 | Comparisons of Extreme Runoff in Different Studies

The extreme low runoff in the central Yangtze River basin is projected to be the most severe and is expected to increase further in the far future compared to the near future, which aligns with the findings regarding projected hydrological drought changes in the severity reported (Gu et al. 2020). Regarding flooding, the relative change results of 100- and 20-year flood quantiles in some GCMs indicated greater changes in eastern and southern China river basins (Gu et al. 2021), which are consistent with the patterns projected for the 90th percentile runoff in this study. However, the drought and flooding analysis conducted by Gu et al. (2020, 2021) was performed under RCP8.5 in CMIP5 and focused on specific basins of China, rather than covering the entire country.

4.3 | The Dominant Driving Forces for Runoff Changes

Runoff changes in the future under climate change primarily stem from alterations in precipitation patterns, temperature variations, shifts in the hydrological cycle, and changes in the land surface. Continuous climate change is expected to increase the variability of the water cycle, leading to more global monsoon precipitation, as well as the occurrence of very wet and very dry weather, climate events and seasons (IPCC 2023). Specifically, in a warming climate, the water vapour holding capacity increases according to the Clausius-Clapeyron law (Clapeyron 1834; Clausius 1850). This results in more precipitable water and intensified precipitation extremes, which may cause flooding events. Warmer temperatures can enhance water evaporation from the ground. As soils desiccate, the overlying air may heat up further, intensifying evaporation and exacerbating drought conditions.

In the case of China, projected runoff changes can be attributed to two key factors: the contribution of precipitation and dominant climatic drivers. First, precipitation plays a significant role in driving runoff changes across most basins in China (Huang et al. 2016; Zhai et al. 2018). In the Southeast and Southwest basins, runoff change patterns are largely influenced by the positive contribution of precipitation, resulting in similar trends across these basins. In contrast, the runoff patterns in the Yellow River and Songhua River basins are shaped by a negative contribution from precipitation, leading to similar runoff behaviours in these basins.

Second, the dominant climatic factors influencing runoff changes vary in different basins. In the lower reaches of the Yangtze River basin, the Pearl River basin, the Huaihe River basin, and the southeast area, net radiation is the primary factor driving runoff changes. Conversely, in the upper reaches of the Yellow River basin and the northern part of the Songhua River basin, air temperature plays a more critical role (Huang et al. 2016). Liu et al. (2017) also found that in the Yellow River and Songhua River basins, a 1% increase in precipitation would lead to a 2%–5% increase in runoff, whilst a 1°C rise in temperature would reduce runoff by 1%–5%.

Floods over mainland China are mainly induced by storm extremes (Wei et al. 2018; Yin et al. 2018), and this is evident in the regional variations in extreme high runoff in this study. Northern regions are expected to experience smaller absolute changes in precipitation extremes, whilst southeastern regions, with significant increases in precipitation extremes (Guo et al. 2018), face a much higher flood risk.

For extreme low runoff, regions projected to experience similar change patterns likely do so due to their shared primary driving factors. Ding et al. (2024) highlighted precipitation as the dominant driver in northwestern China, the North China Plain, and southern China. In contrast, soil moisture plays a more critical role as the primary factor in driving hydrologic drought in southwestern and northeastern China.

4.4 | Uncertainties of the Study

Due to the difficulty in obtaining gauge discharge data in China (Lin et al. 2023), we used open access observational data to calibrate and validate the JULES model. Although the number of sites is limited, the results indicate that the model performs acceptably within the available dataset. If more site data distributed across various regions of China can be obtained and applied to calibration and validation, the model performance could be further improved.

Additionally, this study did not consider the influence of hydraulic structures on runoff, which could potentially alter the distribution of runoff and the occurrence of floods. Our study primarily focuses on understanding the impacts of climate change on hydrological processes. Investigating how hydraulic structures affect such processes is beyond our scope. Consequently, we did not incorporate the effects of hydraulic engineering structures into our model. Future research could involve integrating data on dams, reservoirs, and other hydraulic structures into hydrological models to assess their effects on runoff dynamics. This approach could investigate how human activities impact hydrological processes and contribute to flood vulnerability.

The land surface model and precipitation data products introduce uncertainties into runoff extremes. These uncertainties may increase during the propagation through models when projecting runoff extremes in southeast China, but decrease in north China (Marthews et al. 2020).

GCMs introduce uncertainty into hydrological modelling, and the selection of GCMs can significantly affect the climate change

10970088, 0, Downloaded from https://rmets.onlinelibrary.wiley.com/doi/10.1002/joc.70270 by UK Centre For Ecology & Hydrology, Wiley Online Library on [30/01/2026]. See the Terms and Conditions (https://onlinelibrary.wiley.com/terms-and-conditions) on Wiley Online Library for rules of use; OA articles are governed by the applicable Creative Commons License

impacts on hydrology (Her et al. 2019). Therefore, in this study, three GCMs that are deemed more suitable for China were selected based on their precipitation downscaling performance amongst the six GCMs evaluated. Meanwhile, the ensemble mean values of precipitation and temperature from the three selected GCMs were compared with those from 19 GCMs to ensure the representativeness of the model spread. Whilst using and screening more GCMs for hydrological simulation may help reduce uncertainty, it also necessitates substantial computing resources.

4.5 | Practical Implications

Given the projected increase in runoff depth by 7.30 mm per decade under the high emission scenario, water resource managers should prepare for higher water availability, especially in eastern and southern basins. This information is vital for optimising water storage and distribution systems to prevent wastage and ensure equitable water distribution.

The contrasting seasonal trends between northern and southern China highlight the need for region-specific water management strategies. Whilst southern regions are expected to experience wetter summers, northern regions may face drier conditions. Policymakers should develop flexible, seasonal water allocation plans that account for these divergent trends, optimising water use for agriculture, urban needs, and ecosystem protection.

The projected changes in 90th and 10th percentile runoff suggest a need for enhancing disaster preparedness. Areas prone to flooding should focus on flood defence infrastructure, whilst regions facing drought risk should prioritise sustainable water management and conservation efforts. Coordinating national and local strategies will be key in mitigating the adverse impacts of both extremes.

5 | Conclusions

In this study, we constructed a JULES model specifically tailored for simulating hydrological processes in China and employed the BCSD method to downscale and bias correct the three selected GCMs. Using the GCMs to drive the JULES model, the future hydrological processes under medium and high emission scenarios were projected. The main findings are summarised below:

1. The JULES model performed well in simulating hydrological processes in China at 0.25° resolution. It is particularly well-suited for modelling hydrological processes in Southern China, which is characterised by a humid climate.
2. The contrasting trends in northwestern and southern China suggest differing seasonal patterns, with wetter summers and drier winters projected for the south under the high-emission scenario, whilst the opposite trend is expected in the northwest.
3. More than 56% of area in China, especially in southern China, is projected to experience increased risk of extreme high runoff. Southern regions (Southeast basin, Pearl River basin, and southern Yangtze River basin) are expected to face significantly heightened extreme high runoff. Compared to SSP245, southern regions (Pearl River, Southeast, and Southwest basins) are projected to experience lower risk of extreme high runoff in the near future but significantly higher risk in the far future under SSP585.
4. Conversely, more than 40% of area in China, predominantly in central and southern regions, is projected to experience severe extreme low runoff, which would lead to more severe drought conditions. The area facing extreme low runoff is expected to be wider under SSP245 in the near future, but under SSP585, the drying trend is expected to intensify over time. These findings highlight the influence of different emission scenarios on extreme high and low runoff; it is important to take proactive measures to enhance climate adaptations in the future.

Author Contributions

Danyang Gao: methodology, formal analysis, visualization, writing – original draft. **Toby Richard Marthews:** software, writing – review and editing. **Guangtao Fu:** supervision, writing – review and editing. **Li Zhou:** writing – review and editing. **Fayyaz Ali Memon:** writing – review and editing.

Acknowledgements

We are grateful to Prof. Albert S. Chen, Centre for Water Systems, University of Exeter, for his support and valuable comments to improve the manuscript. Danyang Gao received additional support through the visiting scientist programme under the Hydro-JULES scheme at UK Centre for Ecology & Hydrology (UKCEH) in November 2022. We acknowledge JASMIN super-data-cluster (Lawrence et al. 2012). The running of JULES and analysis of results in this work were performed on the JASMIN. JASMIN is managed and delivered by the UK Science and Technology Facilities Council (STFC) Centre for Environmental Data Archival (CEDA).

Funding

The authors have nothing to report.

Conflicts of Interest

The authors declare no conflicts of interest.

Data Availability Statement

The data that support the findings of this study are available from the corresponding author upon reasonable request.

References

Best, M. J., M. Pryor, D. B. Clark, et al. 2011. "The Joint UK Land Environment Simulator (JULES), Model Description – Part 1: Energy and Water Fluxes." *Geoscientific Model Development* 4, no. 3: 677–699. https://doi.org/10.5194/gmd-4-677-2011.

Bian, G., J. Zhang, J. Chen, et al. 2021. "Projecting Hydrological Responses to Climate Change Using CMIP6 Climate Scenarios for the Upper Huai River Basin, China." *Frontiers in Environmental Science* 9: 759547. https://doi.org/10.3389/fenvs.2021.759547.

Chai, Y., W. R. Berghuijs, K. Naudts, T. A. J. Janssen, Y. Yao, and H. Dolman. 2021. "Using Precipitation Sensitivity to Temperature to

10970088, 0, Downloaded from https://rmets.onlinelibrary.wiley.com/doi/10.1002/joc.70270 by UK Centre For Ecology & Hydrology, Wiley Online Library on [30/01/2026]. See the Terms and Conditions (https://onlinelibrary.wiley.com/terms-and-conditions) on Wiley Online Library for rules of use; OA articles are governed by the applicable Creative Commons License

Adjust Projected Global Runoff." *Environmental Research Letters* 16: 124032. https://doi.org/10.1088/1748-9326/ac3795.

Chen, Y., L. Wang, X. Shi, et al. 2023. "Impact of Climate Change on the Hydrological Regimes of the Midstream Section of the Yarlung Tsangpo River Basin Based on SWAT Model." *Water* 15: 685. https://doi.org/10.3390/w15040685.

Chou, H.-K., A. M. de Heuminski Avila, and M. Bray. 2022. "Evaluating the Atibaia River Hydrology Using JULES6.1." *Geoscientific Model Development* 15: 5233–5240. https://doi.org/10.5194/gmd-15-5233-2022.

Clapeyron, É. 1834. "Mémoire sur la puissance motrice de la chaleur." *Journal De L'école Polytechnique* 23: 153–190.

Clark, D. B., L. M. Mercado, S. Sitch, et al. 2011. "The Joint UK Land Environment Simulator (JULES), Model Description – Part 2: Carbon Fluxes and Vegetation Dynamics." *Geoscientific Model Development* 4, no. 3: 701–722. https://doi.org/10.5194/gmd-4-701-2011.

Clausius, R. 1850. "Ueber die bewegende Kraft der Wärme und die Gesetze, welche sich daraus für die Wärmelehre selbst ableiten lassen." *Annalen der Physik* 155: 500–524. https://doi.org/10.1002/andp.18501550403.

Cook, B. I., J. S. Mankin, K. Marvel, A. P. Williams, J. E. Smerdon, and K. J. Anchukaitis. 2020. "Twenty-First Century Drought Projections in the CMIP6 Forcing Scenarios." *Earth's Future* 8: e2019EF001461. https://doi.org/10.1029/2019EF001461.

Cox, P. M., R. A. Betts, C. B. Bunton, R. L. H. Essery, P. R. Rowntree, and J. Smith. 1999. "The Impact of New Land Surface Physics on the GCM Simulation of Climate and Climate Sensitivity." *Climate Dynamics* 15, no. 3: 183–203. https://doi.org/10.1007/s003820050276.

Cucchi, M., G. P. Weedon, A. Amici, et al. 2020. "WFDE5: Bias-Adjusted ERA5 Reanalysis Data for Impact Studies." *Earth System Science Data* 12: 2097–2120. https://doi.org/10.5194/essd-12-2097-2020.

de la Martínez- Torre, A., E. M. Blyth, and G. P. Weedon. 2019. "Using Observed River Flow Data to Improve the Hydrological Functioning of the JULES Land Surface Model (vn4.3) Used for Regional Coupled Modelling in Great Britain (UKC2)." *Geoscientific Model Development* 12: 765–784. https://doi.org/10.5194/gmd-12-765-2019.

Decharme, B., R. Alkama, F. Papa, S. Faroux, H. Douville, and C. Prigent. 2012. "Global Off-Line Evaluation of the ISBA-TRIP Flood Model." *Climate Dynamics* 38: 1389–1412. https://doi.org/10.1007/s00382-011-1054-9.

Ding, Y., Z. Lu, L. Wu, et al. 2024. "Evaluating the Spatiotemporal Dynamics of Driving Factors for Multiple Drought Types in Different Climate Regions of China." *Journal of Hydrology* 640: 131710. https://doi.org/10.1016/j.jhydrol.2024.131710.

Eyring, V., S. Bony, G. A. Meehl, et al. 2016. "Overview of the Coupled Model Intercomparison Project Phase 6 (CMIP6) Experimental Design and Organization." *Geoscientific Model Development* 9: 1937–1958. https://doi.org/10.5194/gmd-9-1937-2016.

Gu, L., J. Chen, J. Yin, C.-. Y. Xu, and J. Zhou. 2020. "Responses of Precipitation and Runoff to Climate Warming and Implications for Future Drought Changes in China." *Earth's Future* 8: e2020EF001718. https://doi.org/10.1029/2020EF001718.

Gu, L., J. Yin, H. Zhang, et al. 2021. "On Future Flood Magnitudes and Estimation Uncertainty Across 151 Catchments in Mainland China." *International Journal of Climatology* 41: E779–E800. https://doi.org/10.1002/joc.6725.

Guan, X., J. Zhang, Z. Bao, C. Liu, J. Jin, and G. Wang. 2021. "Past Variations and Future Projection of Runoff in Typical Basins in 10 Water Zones, China." *Science of the Total Environment* 798: 149277. https://doi.org/10.1016/j.scitotenv.2021.149277.

Guo, J., G. Huang, X. Wang, Y. Li, and L. Yang. 2018. "Future Changes in Precipitation Extremes Over China Projected by a Regional Climate Model Ensemble." *Atmospheric Environment* 188: 142–156. https://doi.org/10.1016/j.atmosenv.2018.06.026.

Gupta, H. V., S. Sorooshian, and P. O. Yapo. 1999. "Status of Automatic Calibration for Hydrologic Models: Comparison With Multilevel Expert Calibration." *Journal of Hydrologic Engineering* 4: 135–143. https://doi.org/10.1061/(ASCE)1084-0699(1999)4:2(135).

Her, Y., S.-H. Yoo, J. Cho, S. Hwang, J. Jeong, and C. Seong. 2019. "Uncertainty in Hydrological Analysis of Climate Change: Multi-Parameter vs. Multi-GCM Ensemble Predictions." *Scientific Reports* 9: 4974. https://doi.org/10.1038/s41598-019-41334-7.

Hersbach, H., B. Bell, P. Berrisford, et al. 2020. "The ERA5 Global Reanalysis." *Quarterly Journal of the Royal Meteorological Society* 146: 1999–2049. https://doi.org/10.1002/qj.3803.

Huang, Z., H. Yang, and D. Yang. 2016. "Dominant Climatic Factors Driving Annual Runoff Changes at the Catchment Scale Across China." *Hydrology and Earth System Sciences* 20: 2573–2587. https://doi.org/10.5194/hess-20-2573-2016.

Ingabire, R., Y. Chang, X. Liu, B. Cao, A. Umugwaneza, and Y. Shen. 2024. "Comparative Assessment of Impacts of Future Climate Change on Runoff in Upper Daqinghe Basin, China." *Chinese Geographical Science* 34: 564–578. https://doi.org/10.1007/s11769-024-1433-x.

IPCC. 2023. *Climate Change 2023: Synthesis Report. Contribution of Working Groups I, II and III to the Sixth Assessment Report of the Intergovernmental Panel on Climate Change*. Intergovernmental Panel on Climate Change (IPCC).

Jia, Q., H. Jia, Y. Li, and D. Yin. 2023. "Applicability of CMIP5 and CMIP6 Models in China: Reproducibility of Historical Simulation and Uncertainty of Future Projection." *Journal of Climate* 36: 5809–5824. https://doi.org/10.1175/JCLI-D-22-0375.1.

Jin, H., X. Chen, P. Wu, C. Song, and W. Xia. 2021. "Evaluation of Spatial-Temporal Distribution of Precipitation in Mainland China by Statistic and Clustering Methods." *Atmospheric Research* 262: 105772. https://doi.org/10.1016/j.atmosres.2021.105772.

Kendall, M. G. 1975. *Rank Correlation Methods*. 4th ed. Griffin.

Lawrence, B. N., V. Bennett, and J. Churchill. 2012. The JASMIN Super-Data-Cluster.

Le Vine, N., A. Butler, N. McIntyre, and C. Jackson. 2016. "Diagnosing Hydrological Limitations of a Land Surface Model: Application of JULES to a Deep-Groundwater Chalk Basin." *Hydrology and Earth System Sciences* 20: 143–159. https://doi.org/10.5194/hess-20-143-2016.

Li, M., H. Wang, H. Gu, B. Chi, and Y. Li. 2025. "Future Runoff in Anthropogenic Areas Under Climate Change: The Semi-Arid Liuhe Basin, China." *Theoretical and Applied Climatology* 156: 235. https://doi.org/10.1007/s00704-025-05465-4.

Lin, J., B. A. Bryan, X. Zhou, et al. 2023. "Making China's Water Data Accessible, Usable and Shareable." *Nature Water* 1: 328–335. https://doi.org/10.1038/s44221-023-00039-y.

Liu, J., Q. Zhang, Y. Zhang, X. Chen, J. Li, and S. K. Aryal. 2017. "Deducing Climatic Elasticity to Assess Projected Climate Change Impacts on Streamflow Change Across China." *Journal of Geophysical Research: Atmospheres* 122: 10,228–10,245. https://doi.org/10.1002/2017JD026701.

Lu, K., M. Arshad, X. Ma, I. Ullah, J. Wang, and W. Shao. 2022. "Evaluating Observed and Future Spatiotemporal Changes in Precipitation and Temperature Across China Based on CMIP6-GCMs." *International Journal of Climatology* 42: 7703–7729. https://doi.org/10.1002/joc.7673.

Mann, H. B. 1945. "Nonparametric Tests Against Trend." *Econometrica* 13: 245–259. https://doi.org/10.2307/1907187.

Marthews, T. R., E. M. Blyth, A. de la Martínez- Torre, and T. I. E. Veldkamp. 2020. "A Global-Scale Evaluation of Extreme Event

10970088, 0, Downloaded from https://rmets.onlinelibrary.wiley.com/doi/10.1002/joc.70270 by UK Centre For Ecology & Hydrology, Wiley Online Library on [30/01/2026]. See the Terms and Conditions (https://onlinelibrary.wiley.com/terms-and-conditions) on Wiley Online Library for rules of use; OA articles are governed by the applicable Creative Commons License

Uncertainty in the *eartH2Observe* Project." *Hydrology and Earth System Sciences* 24: 75–92. https://doi.org/10.5194/hess-24-75-2020.

Marthews, T. R., S. J. Dadson, D. B. Clark, et al. 2022. "Inundation Prediction in Tropical Wetlands From JULES-CaMa-Flood Global Land Surface Simulations." *Hydrology and Earth System Sciences* 26: 3151–3175. https://doi.org/10.5194/hess-26-3151-2022.

Miao, C., Y. Wu, X. Fan, and J. Su. 2023. "Projections of Global Land Runoff Changes and Their Uncertainty Characteristics During the 21st Century." *Earth's Future* 11: e2022EF003286. https://doi.org/10.1029/2022EF003286.

Miller, O. L., M. P. Miller, P. C. Longley, et al. 2021. "How Will Baseflow Respond to Climate Change in the Upper Colorado River Basin?" *Geophysical Research Letters* 48: e2021GL095085. https://doi.org/10.1029/2021GL095085.

Mo, C., M. Bao, S. Lai, et al. 2023. "Impact of Future Climate and Land Use Changes on Runoff in a Typical Karst Basin, Southwest China." *Water* 15: 2240. https://doi.org/10.3390/w15122240.

Murphy, J. M., D. M. H. Sexton, D. N. Barnett, et al. 2004. "Quantification of Modelling Uncertainties in a Large Ensemble of Climate Change Simulations." *Nature* 430: 768–772. https://doi.org/10.1038/nature02771.

Nash, J. E., and J. V. Sutcliffe. 1970. "River Flow Forecasting Through Conceptual Models Part I—A Discussion of Principles." *Journal of Hydrology* 10: 282–290. https://doi.org/10.1016/0022-1694(70)90255-6.

Schewe, J., J. Heinke, D. Gerten, et al. 2014. "Multimodel Assessment of Water Scarcity Under Climate Change." *Proceedings of the National Academy of Sciences* 111: 3245–3250. https://doi.org/10.1073/pnas.1222460110.

Singh, D., M. Vardhan, R. Sahu, D. Chatterjee, P. Chauhan, and S. Liu. 2023. "Machine-Learning- and Deep-Learning-Based Streamflow Prediction in a Hilly Catchment for Future Scenarios Using CMIP6 GCM Data." *Hydrology and Earth System Sciences* 27: 1047–1075. https://doi.org/10.5194/hess-27-1047-2023.

Song, X., M. Xu, S. Kang, R. Wang, and H. Wu. 2024. "Evaluation and Projection of Changes in Temperature and Precipitation Over Northwest China Based on CMIP6 Models." *International Journal of Climatology* 44: 5039–5056. https://doi.org/10.1002/joc.8622.

Sun, H., F. Su, T. Yao, et al. 2021. "General Overestimation of ERA5 Precipitation in Flow Simulations for High Mountain Asia Basins." *Environmental Research Communications* 3: 121003. https://doi.org/10.1088/2515-7620/ac40f0.

Thrasher, B., W. Wang, A. Michaelis, F. Melton, T. Lee, and R. Nemani. 2022. "NASA Global Daily Downscaled Projections, CMIP6." *Sci Data* 9: 262. https://doi.org/10.1038/s41597-022-01393-4.

Wang, A., Y. Miao, X. Kong, and H. Wu. 2022. "Future Changes in Global Runoff and Runoff Coefficient From CMIP6 Multi-Model Simulation Under SSP1-2.6 and SSP5-8.5 Scenarios." *Earth's Future* 10: e2022EF002910. https://doi.org/10.1029/2022EF002910.

Wang, Y., X. Yang, M. Zhang, et al. 2019. "Projected Effects of Climate Change on Future Hydrological Regimes in the Upper Yangtze River Basin, China." *Advances in Meteorology* 2019: 1545746. https://doi.org/10.1155/2019/1545746.

Wei, L., K. Hu, and X. Hu. 2018. "Rainfall Occurrence and Its Relation to Flood Damage in China From 2000 to 2015." *Journal of Mountain Science* 15: 2492–2504. https://doi.org/10.1007/s11629-018-4931-4.

Wood, A. W., L. R. Leung, V. Sridhar, and D. P. Lettenmaier. 2004. "Hydrologic Implications of Dynamical and Statistical Approaches to Downscaling Climate Model Outputs." *Climatic Change* 62: 189–216. https://doi.org/10.1023/B:CLIM.0000013685.99609.9e.

Xu, Z., Y. Han, C.-Y. Tam, Z. L. Yang, and C. Fu. 2021. "Bias-Corrected CMIP6 Global Dataset for Dynamical Downscaling of the Historical and Future Climate (1979–2100)." *Scientific Data* 8: 293. https://doi.org/10.1038/s41597-021-01079-3.

Xue, P., C. Zhang, Z. Wen, F. Yu, E. Park, and V. Nourani. 2024. "Climate Variability Impacts on Runoff Projection in the 21st Century Based on the Applicability Assessment of Multiple GCMs: A Case Study of the Lushi Basin, China." *Journal of Hydrology* 638: 131383. https://doi.org/10.1016/j.jhydrol.2024.131383.

Yang, H., C. Huntingford, A. Wiltshire, S. Sitch, and L. Mercado. 2019. "Compensatory Climate Effects Link Trends in Global Runoff to Rising Atmospheric CO2 Concentration." *Environmental Research Letters* 14: 124075. https://doi.org/10.1088/1748-9326/ab5c6f.

Yang, L., G. Zhao, P. Tian, et al. 2022. "Runoff Changes in the Major River Basins of China and Their Responses to Potential Driving Forces." *Journal of Hydrology* 607: 127536. https://doi.org/10.1016/j.jhydrol.2022.127536.

Yang, X., B. Zhou, Y. Xu, and Z. Han. 2021. "CMIP6 Evaluation and Projection of Temperature and Precipitation Over China." *Advances in Atmospheric Sciences* 38: 817–830. https://doi.org/10.1007/s00376-021-0351-4.

Yin, J., P. Gentine, S. Zhou, et al. 2018. "Large Increase in Global Storm Runoff Extremes Driven by Climate and Anthropogenic Changes." *Nature Communications* 9: 4389. https://doi.org/10.1038/s41467-018-06765-2.

Zhai, R., F. Tao, Y. Chen, H. Dai, Z. Liu, and B. Fu. 2022. "Future Water Security in the Major Basins of China Under the 1.5°C and 2.0°C Global Warming Scenarios." *Science of the Total Environment* 849: 157928. https://doi.org/10.1016/j.scitotenv.2022.157928.

Zhai, R., F. Tao, and Z. Xu. 2018. "Spatial–Temporal Changes in Runoff and Terrestrial Ecosystem Water Retention Under 1.5 and 2°C Warming Scenarios Across China." *Earth System Dynamics* 9: 717–738. https://doi.org/10.5194/esd-9-717-2018.

Zhang, X., Q. Tang, X. Liu, G. Leng, and C. Di. 2018. "Nonlinearity of Runoff Response to Global Mean Temperature Change Over Major Global River Basins." *Geophysical Research Letters* 45: 6109–6116. https://doi.org/10.1029/2018GL078646.

Zhang, Z., X. Chen, C.-Y. Xu, L. Yuan, B. Yong, and S. Yan. 2011. "Evaluating the Non-Stationary Relationship Between Precipitation and Streamflow in Nine Major Basins of China During the Past 50 Years." *Journal of Hydrology* 409: 81–93. https://doi.org/10.1016/j.jhydrol.2011.07.041.

Zhao, Q., Y. Ding, J. Wang, et al. 2019. "Projecting Climate Change Impacts on Hydrological Processes on the Tibetan Plateau With Model Calibration Against the Glacier Inventory Data and Observed Streamflow." *Journal of Hydrology* 573: 60–81. https://doi.org/10.1016/j.jhydrol.2019.03.043.

Zhou, J., H. Lu, K. Yang, et al. 2023. "Projection of China's Future Runoff Based on the CMIP6 Mid-High Warming Scenarios." *Science China Earth Sciences* 66: 528–546. https://doi.org/10.1007/s11430-022-1055-5.

Zhou, Z., S. Chen, Z. Li, and Y. Luo. 2023. "An Evaluation of CRA40 and ERA5 Precipitation Products Over China." *Remote Sensing* 15: 5300. https://doi.org/10.3390/rs15225300.

Zulkafli, Z., W. Buytaert, C. Onof, W. Lavado, and J. L. Guyot. 2013. "A Critical Assessment of the JULES Land Surface Model Hydrology for Humid Tropical Environments." *Hydrology and Earth System Sciences* 17: 1113–1132. https://doi.org/10.5194/hess-17-1113-2013.

Supporting Information

Additional supporting information can be found online in the Supporting Information section. **Data S1:** Supporting Information.

10970088, 0, Downloaded from https://rmets.onlinelibrary.wiley.com/doi/10.1002/joc.70270 by UK Centre For Ecology & Hydrology, Wiley Online Library on [30/01/2026]. See the Terms and Conditions (https://onlinelibrary.wiley.com/terms-and-conditions) on Wiley Online Library for rules of use; OA articles are governed by the applicable Creative Commons License